Atomic ground states in strong magnetic fields: electron configurations and energy levels

Christoph Schimeczek, Sebastian Boblest, Dirk Meyer, and Günter Wunner
Institut für Theoretische Physik 1, Universität Stuttgart, D-70550 Stuttgart, Germany
(Dated: May 22, 2013)

Using a combination of a fast 2D-Hartree-Fock-Roothaan method and highly accurate Fixed-Phase Diffusion Quantum Monte Carlo simulations, we analyze the electronic structure and calculate the energy of the ground states of atoms with nuclear charges $Z = 2 - 26$ in very strong magnetic fields $B = 10^7\,\mathrm{T} - 5 \cdot 10^8\,\mathrm{T}$, relevant for astrophysical problems, e.g. the thermal emission of strongly magnetized isolated neutron stars.

PACS numbers: 31.15.xr, 31.15.ag, 32.60.+i, 71.10.-w

I. INTRODUCTION

Over the last decade continuing effort has gone into calculating, with ever increasing accuracy and with various methods, the energies of atoms and ions in neutron star magnetic fields. The motivation comes largely from the fact that features discovered [1–3] in the thermal emission spectra of isolated neutron stars may be due to absorption of photons by heavy atoms in the hot, thin atmospheres of these strongly magnetized cosmic objects [4]. Also, features of heavier elements may be present in the spectra of magnetic white dwarf stars [5, 6].

While comprehensive and precise data for hydrogen in strong magnetic fields have been available for some time (cf. [7–10]), this is less the case for atoms and ions with more than one electron. Accurate ground state energies of atoms up to nuclear charge $Z = 10$ in the high-field regime were first determined by Ivanov and Schmelcher [11] who solved the 2D-Hartree-Fock equations on a flexible mesh. By means of a specific multiconfigurational perturbative hybrid Hartree-Hartree-Fock method Mori and Hailey [12] computed the energies of low-lying states in strong magnetic fields for atoms up to $Z = 26$. In another Hartree-Fock approach Thirumalai and Heyl [13] obtained very accurate values for the low-lying levels of helium. Low-lying states of lithium and beryllium have been studied with high accuracy using modified freezing full-core methods [14, 15], configuration interaction methods [16, 17], and methods based on an anisotropic Gaussian basis set [18–20].

Along a different line of approach, Monte Carlo methods from ab initio quantum chemistry [21] have also been proven to be a powerful tool for the very accurate computation of the energy values of the ground states of all elements up to iron ($Z = 26$) in magnetic fields $B = 10^7\,\mathrm{T}$ - $5 \cdot 10^8\,\mathrm{T}$ [22], and, restricted so far to helium, also of the energies of low-lying excited states [23, 24]. These methods use precalculated Hartree-Fock wave functions as guiding wave functions for the diffusion quantum Monte Carlo step, and include correlations via Jastrow factors.

In Ref. [22] the guiding wave functions were determined using the adiabatic approximation, which amounts to taking single-particle orbitals as products of a Landau wave function for the quantum mechanical description of the (fast) motion of the electron perpendicular to the direction of the magnetic field, and a longitudinal wave function for the (slow) motion along the field. This approximation limits the applicability of the method to magnetic fields where the nuclear charge scaled magnetic field parameter $\beta_Z = B/(B_0 Z^2)$ (with $B_0 = 4.70103 \cdot 10^5\,\mathrm{T}$) is much larger than 1. (At B_0, the electron's Larmor-radius becomes equal to the Bohr radius of the hydrogen atom).

The purpose of this paper is to abandon this approximation, and in this way to extend the range of applicability of quantum Monte Carlo calculations for atoms in strong magnetic fields down towards the regime of intermediate field strengths. We do this by choosing a more sophisticated ansatz for the single-particle orbitals in the Hartree-Fock step for the guiding wave functions that precedes the quantum Monte Carlo procedure.

In very strong magnetic fields the spin of all electrons can be assumed to be aligned opposite to the direction of the magnetic field because of the large spin flip energies. This is no longer true when the magnetic field decreases. We also include states without full spin-alignment and can indeed demonstrate that for $Z > 10$ in a field with $B = 10^7\,\mathrm{T}$ and for $Z > 21$ at $B = 5 \cdot 10^7\,\mathrm{T}$ the ground state configurations contain an electron with spin parallel to the magnetic field, contrary to the assumptions made in earlier calculations [22].

The paper is organized as follows. In Sec. II we give a brief summary of the 2D-Hartree-Fock-Roothaan (2DHFR) method, and recapitulate the Fixed-Phase Diffusion Quantum Monte Carlo (FPDQMC) method in Sec. III. Section IV contains a comparison of our results for ground state energies and oscillator strengths with previous work in the literature. We conclude with a summary and an outlook in Sec. V.

II. THE 2DHFR METHOD

A. 2D-Hartree-Fock-Roothaan equations

Since we restrict ourselves to strong magnetic fields $\beta_Z \geq 0.1$ we use cylindrical coordinates and atomic Rydberg units for the many particle Hamiltonian

$$\hat{H} = \sum_{i=1}^{N} \Big(-\Delta_i - 2\mathrm{i}\beta\partial_{\varphi_i} + \beta^2\rho_i^2 + 4\beta m_{\mathrm{s}_i} - 2\frac{Z}{|\boldsymbol{r}_i|} + \sum_{j=i+1}^{N} \frac{2}{|\boldsymbol{r}_i - \boldsymbol{r}_j|} \Big) \tag{1}$$

of a non-moving, N-electron atomic system in a magnetic field pointing in z-direction with infinite mass of the nucleus of charge Z. Flipping a single electron spin m_{s} equals 4β in Rydberg energies, so for very high magnetic fields we expect full spin-down polarization, while for intermediate field strengths the spin of a few electrons may point "up" to gain access to low-lying single-particle orbitals that are already occupied with spin-down electrons.

The many particle wave function Ψ is constructed from two Slater-determinants of single particle wave functions ψ^i for each electron i – one for all spin-up electrons and one for all spin-down electrons. These Slater-determinants are then combined in a Hartree-Product.

In a previous version of the Hartree-Fock-Roothaan method [25, 26] the single-electron orbitals were taken in the form of a product,

$$\tilde{\psi}^i(\rho_i, \varphi_i, z_i) = P^i(z_i) \sum_{n=0}^{N_{\mathrm{L}}} t_n^i \, \Phi_{nm_i}(\rho_i, \varphi_i) \,, \tag{2}$$

a sum over the $N_{\mathrm{L}}+1$ Landau states $\Phi_{nm_i}(\rho, \varphi)$, weighted by an occupation vector t_n^i, and a Landau quantum number independent longitudinal wave function $P^i(z_i)$

In this work we go beyond the product ansatz in equation (2) and proceed to a full 2D-description of the problem with individual longitudinal wave functions $P_n^i(z_i)$ for each Landau level

$$\psi^i(\rho_i, \varphi_i, z_i) = \sum_{n=0}^{N_{\mathrm{L}}} P_n^i(z_i) \, \Phi_{nm_i}(\rho_i, \varphi_i). \tag{3}$$

As an example Figure 1 shows that the longitudinal wave functions $P_n^i(z_i)$ corresponding to the Landau levels Φ_{nm_i} differ considerably for magnetic field strengths $\beta_Z \lesssim 1$, thus our ansatz (3) will allow for a much better description of the wave functions.

The z-wave functions

$$P_n^i(z_i) = \sum_{\nu} \alpha_{n\nu}^i B_\nu^i(z_i) \tag{4}$$

are expanded using individual B-spline [27] bases $B_\nu^i(z_i)$ for each electron, as described in [25, 26]. The variation of the energy functional with respect to the B-spline coefficients $\alpha_{n\nu}^i$ yields two-dimensional Hartree-Fock-Roothaan equations

$$\sum_{n'\mu} F_{n\nu n'\mu}^i \alpha_{n'\mu}^i = \varepsilon_i \sum_{n'\mu} S_{n\nu n'\mu}^i \alpha_{n'\mu}^i, \tag{5}$$

with $F_{n\nu n'\mu}^i$ and $S_{n\nu n'\mu}^i$ being the Fock matrix and the overlap matrix, respectively. The Fock matrix is the sum of the longitudinal and transverse kinetic energy, the nueclear potential energy, as well as the direct and exchange electron-electron energy matrices

$${}^{\mathrm{long}}F_{n\nu n'\mu}^i = -\delta_{n,n'} \int_{-\infty}^{\infty} B_\nu^i(z_i) \frac{\partial^2}{\partial z_i^2} B_\mu^i(z_i) \, \mathrm{d}z_i, \tag{6}$$

$${}^{\mathrm{tran}}F_{n\nu n'\mu}^i = 4n\beta\delta_{n,n'} \int_{-\infty}^{\infty} B_\nu^i(z_i) \, B_\mu^i(z_i) \, \mathrm{d}z_i, \tag{7}$$

$${}^{\mathrm{nucl}}F_{n\nu n'\mu}^i = \int_{-\infty}^{\infty} B_\nu^i(z_i) \, V_{nn'}^i(z_i) \, B_\mu^i(z_i) \, \mathrm{d}z_i, \tag{8}$$

$${}^{\mathrm{dir}}F_{n\nu n'\mu}^i = \sum_{j=1}^{N} \frac{1}{\xi^j} \sum_{k,k'}^{N_{\mathrm{int}}^j} \int_{-\infty}^{\infty} B_\nu^i(z_i) \, B_\mu^i(z_i) \int_{-\infty}^{\infty} P_k^j(z_j) \, U_{nn'kk'}^{ij}(z_i, z_j) \, P_{k'}^j(z_j) \, \mathrm{d}z_j \, \mathrm{d}z_i, \tag{9}$$

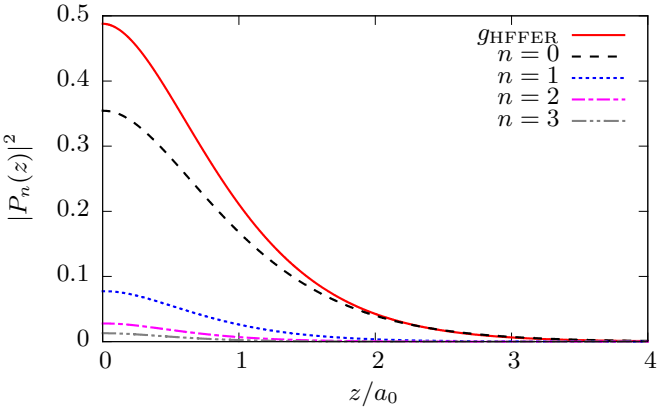

FIG. 1. (Color online) Squared z-wave functions $|P_n(z)|^2$ (maxima normed to one) corresponding to the first four Landau states for the hydrogen ground state at $B = 10^5$ T compared to $|P(z)|^2$ (g_{HFFER}) obtained with our previous ansatz (2).

$$ {}^{\mathrm{ex}}F^i_{n\nu n'\mu} = -\sum_{j=1}^{N} \delta_{m_{\mathrm{s}_i},m_{\mathrm{s}_j}} \frac{1}{\xi^j} \sum_{k,k'}^{N^j_{\mathrm{int}}} \int_{-\infty}^{\infty} B^i_\nu(z_i)\, P^j_k(z_i) \int_{-\infty}^{\infty} B^i_\mu(z_j)\, A^{ij}_{nn'kk'}(z_i,z_j)\, P^j_{k'}(z_j)\, \mathrm{d}z_j\, \mathrm{d}z_i. \tag{10} $$

Explicit forms of the effective potentials $V^i_{nn'}(z_i)$, $U^{ij}_{nn'kk'}(z_i,z_j)$ and $A^{ij}_{nn'kk'}(z_i,z_j)$ can be found in [25], along with a description of their computation. They are precalculated to a precision of 8 digits to speed up the evaluation of the integrals. The parameters ξ^j and N^j_{int} will explained in detail in the next subsection. The overlap matrix can be calculated using

$$ S^i_{n\nu n'\mu} = \delta_{n,n'} \int_{-\infty}^{\infty} B^i_\nu(z_i)\, B^i_\mu(z_i)\, \mathrm{d}z_i. \tag{11} $$

To avoid convergence problems and to reduce the number of iterations, we use the results obtained with our HFFER II code [26] as initial wave functions and solve equations (5) self-consistently.

B. Interaction cutoff & convergence

In the regime of intermediate magnetic field strengths $\beta_Z \lesssim 1$, single-electron states close to the nucleus and its spherical symmetric Coulomb potential are not easily described using only a few Landau states in the cylindrically symmetric expansion (3). This problem occurs for states with magnetic quantum numbers $|m| \lesssim 5$, and especially for states with $m = 0$, whose probability distributions have a finite cusp at $\rho = 0$. Entering this regime therefore requires to blow up the Landau expansion considerably. We increased the number of included Landau levels from $N_{\mathrm{L}} = 7$ in the previous application of the Hartree-Fock-Roothaan method to $N_{\mathrm{L}} = 30$ in this work. However, a complete evaluation of the energy functional would require the calculation of roughly $N \cdot (N_{\mathrm{L}})^4$ electron interaction terms in (9) and (10), causing an unacceptable loss of efficiency. We bypass this problem by introducing the cutoff parameters N^i_{int}, dropping higher Landau level interaction terms in equations (9), (10) between electron i and j with $k, k' > N^j_{\mathrm{int}}$ or $n, n' > N^i_{\mathrm{int}}$, but include all N_{L} Landau levels in eq. (8). We thereby induce a new cutoff error in our energy functional, lowering its miminum value and depriving it of its variational nature, since the repulsive Coulomb interactions are not fully taken into account anymore. To reduce this error we compensate for the loss of the energy contributions due to the repulsive electron-electron interaction by renormalizing the lower Landau levels' interaction terms in (9) and (10) with a factor

$$ \xi^j = \sum_{k>N^j_{\mathrm{int}}}^{N_{\mathrm{L}}} \int_{-\infty}^{\infty} |P^j_k(z_j)|^2\, \mathrm{d}z_j. \tag{12} $$

We implemented a simple Monte Carlo integration algorithm (not the FPDQMC method discussed later) with a correct evaluation of the electron-electron interaction terms ($N^i_{\mathrm{int}} = N^j_{\mathrm{int}} = N_{\mathrm{L}}$) to double-check the results obtained with this modified energy functional. With the help of this algorithm we are able to show that the new cutoff-induced energy error is negligible, as long as the occupation of the higher Landau expansion terms stays small. This is the case for all single particle wave functions when $\beta_Z \gtrsim 0.1$.

Choosing a proper interaction cutoff parameter N^i_{int} for each electron is crucial, both for the speed of the algorithm and for the quality of the results. The optimal N^i_{int} strongly depends on β_Z and the quantum numbers of the wave function ψ^i. By the use of the Landau level occupation vector t^i_n from the inital wave functions obtained with our previous implementation [26], we can predict reasonable parameters N^i_{int} for each electron. We found $(t^i_{N_{\mathrm{int}}})^2 \approx 10^{-6}$ to be a reliable criterion for the cutoff parameter.

Figure 2 shows the change in the computed ground state energy of neutral iron at $B = 5{\cdot}10^7$ T when the Landau expansion order N_{L} of the single particle wave functions is increased (solid red line). The convergence of our ansatz (3) is clearly visible. The simple Monte Carlo corrected energies (blue points with error bars) correspond to the unmodified energy functionals and are at most 2.2 Ry or 0.6‰ above the 2DHFR results. The statistical error of these Monte Carlo results is very small, thus the error bars are hardly visible. At $N_{\mathrm{L}} = 30$ the gap to the FPDQMC-result (dotted orange line) has decreased to less than 7‰, which means an improvement compared to our previous HFFER result (dashed green line) of about 166 Ry or 46‰. Since the electron-electron interaction potentials are precalculated only up to $N^i_{\mathrm{int}} = 7$, the small cutoff error is unavoidable, unless we restrict ourselves to $N_{\mathrm{L}} = 7$. However, this yields a result 100 Ry off current method's value, as is indicated by the black arrow.

III. ESSENTIALS OF FPDQMC

For the reader's convenience, we briefly recapitulate the essentials of the FPDQMC-method. More detailed discussions of DQMC can be found, e.g., in Refs. [28, 29].

DQMC is a projector method based on the simulation of the importance sampled imaginary-time ($\tau = \mathrm{i}t$) Schrödinger equation

$$ \frac{\partial f(\boldsymbol{R},\tau)}{\partial \tau} = \frac{1}{2}\Delta f(\boldsymbol{R},\tau) - \frac{1}{2}\nabla\cdot\left(f(\boldsymbol{R},\tau)\boldsymbol{F}_{\mathrm{Q}}(\boldsymbol{R})\right) - \left(E_{\mathrm{L}}(\boldsymbol{R}) - E_{\mathrm{off}}\right) f(\boldsymbol{R},\tau). \tag{13} $$

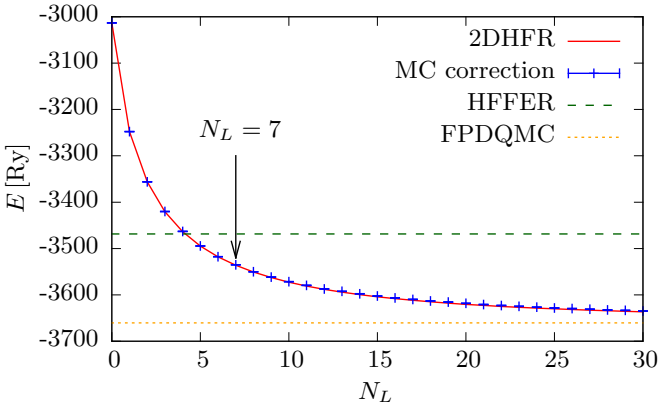

FIG. 2. (Color online) Ground state energy of neutral iron at $B = 5 \cdot 10^7$ T calculated with the 2DHFR-method for different orders N_L of the Landau expansion. Simple Monte Carlo calculations comfirm the smallness of the energy error induced by the reduced electron-electron interactions. Results of our previous method (HFFER) with $N_\mathrm{L} = 7$ and of the accurate FPDQMC-procedure are shown as well.

Here, $\boldsymbol{R} = (\boldsymbol{r}_1, \ldots \boldsymbol{r}_N)$ is a position vector in full configuration space, the sampled density

$$f(\boldsymbol{R}, \tau) \equiv \Psi_\mathrm{G}(\boldsymbol{R}) \Psi(\boldsymbol{R}, \tau) \tag{14}$$

is a product of an arbitrary function $\Psi(\boldsymbol{R}, \tau)$ and the guiding function $\Psi_\mathrm{G}(\boldsymbol{R})$, while $\boldsymbol{F}_\mathrm{Q}(\boldsymbol{R}) = 2\nabla\Psi_\mathrm{G}(\boldsymbol{R})/\Psi_\mathrm{G}(\boldsymbol{R})$ is the quantum force and $E_\mathrm{L}(\boldsymbol{R}) = \hat{H}\Psi_\mathrm{G}(\boldsymbol{R})/\Psi_\mathrm{G}(\boldsymbol{R})$ the local energy. The energy offset E_off is introduced to increase the stability of the simulation and is continuously adapted to the current best estimate of the true ground state energy. By expanding the function Ψ in the basis of eigenfunctions $\{\Psi_i\}$ of $\hat{H}$, i.e.

$$\Psi(\boldsymbol{R}, \tau) = \sum_{i=0}^{\infty} c_i \Psi_i(\boldsymbol{R}) \mathrm{e}^{-(E_i - E_\mathrm{off})\tau}, \tag{15}$$

one sees that contributions of excited states are exponentially suppressed with increasing τ, and only low-lying state contributions remain after a sufficient number of steps in imaginary time. Equation (13) is rewritten in integral form

$$f(\boldsymbol{R}', \tau + \Delta\tau) = \int G(\boldsymbol{R}', \boldsymbol{R}, \Delta\tau) f(\boldsymbol{R}, \tau) \mathrm{d}^{3N} R \tag{16}$$

and the Green's function is written in short-time approximation as $G = G_\mathrm{D} G_\mathrm{B} + \mathcal{O}\left(\delta\tau^2\right)$, where

$$G_\mathrm{D}(\boldsymbol{R}', \boldsymbol{R}; \delta\tau) = \frac{\exp\left[\frac{-(\boldsymbol{R}' - \boldsymbol{R} - \delta\tau \boldsymbol{F}_\mathrm{Q}(\boldsymbol{R})/2)^2}{2\delta\tau}\right]}{(2\pi\delta\tau)^{3N/2}} \tag{17}$$

and

$$G_\mathrm{B}(\boldsymbol{R}', \boldsymbol{R}; \delta\tau) = \exp\left[-\left(\frac{E_\mathrm{L}(\boldsymbol{R}) + E_\mathrm{L}(\boldsymbol{R}')}{2} - E_\mathrm{off}\right)\delta\tau\right]. \tag{18}$$

This integral equation can be simulated in configuration space with an ensemble of random walkers. Each walker moves according to $\boldsymbol{R} = \boldsymbol{R}' + \boldsymbol{\eta} + 2\delta\tau \boldsymbol{F}(\boldsymbol{R}')$, where $\boldsymbol{\eta}$ is a vector of Gaussian distributed random numbers (mean $\mu = 0$, variance $\sigma^2 = \delta\tau$). After each step $C = \mathrm{trunc}\left(G_\mathrm{B}(\boldsymbol{R}, \boldsymbol{R}'; \delta\tau) + \chi\right)$ copies of each walker are created, where $\chi \in [0, 1)$ is a uniform random variate. In all following steps, these C copies move independently.

We note that FPDQMC strictly uses two different functions constructed from the Hartree-Fock results. First the guiding function $\Psi_\mathrm{G}(\boldsymbol{R})$ that is used to determine the movement of the ensemble and the creation of walkers, as outlined above. Second the trial function $\Psi_\mathrm{T}(\boldsymbol{R})$ that is used to evaluate the energy estimate. As is usual in FPDQMC, we take the choice $\Psi_\mathrm{G}(\boldsymbol{R}) = |\Psi_\mathrm{T}(\boldsymbol{R})|$.

In the presence of a magnetic field, the time reversal invariance of the Hamiltonian is broken, and the ground state may be complex. The fixed-phase variant of DQMC introduced in [30] is designed for the treatment of this situation. The initial function is split into its modulus and its phase via

$$\Psi(\boldsymbol{R}, \tau) = |\Psi(\boldsymbol{R}, \tau)| \mathrm{e}^{\mathrm{i}\phi(\boldsymbol{R}, \tau)}. \tag{19}$$

With the help of this ansatz the Schrödinger equation can be split into two coupled differential equations for the modulus and the phase:

$$\left(\sum_{j=1}^{N_\mathrm{e}} -\frac{1}{2}\Delta_j + \frac{1}{2}\left(\boldsymbol{\nabla}_j \phi + \boldsymbol{A}_j\right)^2 + V(\boldsymbol{r}_j)\right)|\Psi| = 0 \tag{20a}$$

$$\sum_{j=1}^{N_\mathrm{e}} \boldsymbol{\nabla}_j \cdot \left[|\Psi|^2 \left(\boldsymbol{\nabla}_j \phi + \boldsymbol{A}_j\right)\right] = 0. \tag{20b}$$

In the fixed phase approximation, Eq. (20b) is assumed to be solved by the phase of the trial function Ψ_T and Eq. (20a) is solved under this assumption.

In recent years, progress has been made in overcoming the fixed-phase approximation, see e.g. [31, 32]. However, these methods are computationally much more expensive.

A. Properties of the trial functions

The trial function $\Psi_\mathrm{T}(\boldsymbol{R}) = \mathcal{J}\Psi_\mathrm{HF}(\boldsymbol{R})$ is a product of the 2DHFR-result $\Psi_\mathrm{HF}(\boldsymbol{R})$ and a Padé-Jastrow factor [21] $\mathcal{J} = \exp(-u)$, with $u = u_\mathrm{Ne} + u_\mathrm{ee}$, where

$$u_\mathrm{Ne} = \sum_{i=1}^{N} \frac{Z\, r_i}{1 + b_\mathrm{Ne}\, r_i}, \tag{21}$$

is the electron-nucleus part and

$$u_\mathrm{ee} = \sum_{j<i}^{N} \sum_{i=1}^{N} \frac{a_{ij}\, r_{ij}}{1 + b_\mathrm{ee}\, r_{ij}}, \tag{22}$$

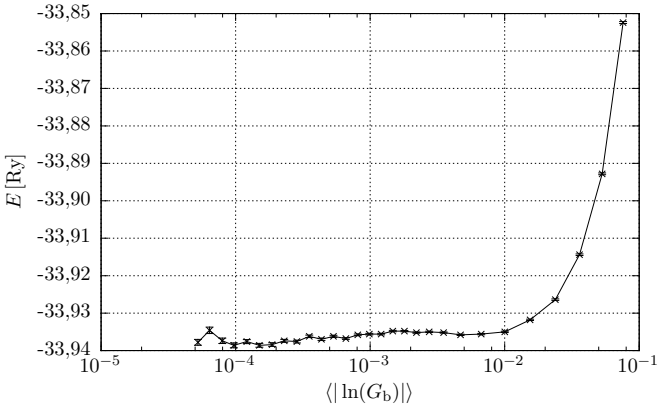

FIG. 3. Time step error for the helium state $(0,0)\,(1,0)$ at $B = 5 \cdot 10^7$ T as a function of $\langle|\ln(G_{\mathrm{B}})|\rangle$.

the electron-electron part, with $a_{ij} = -1/4$ for electrons with parallel spin and $a_{ij} = -1/2$ for electrons with antiparallel spin.

The two free parameters b_{Ne} and b_{ee} are optimized in a two-dimensional scheme using a variational quantum Monte Carlo algorithm with correlated sampling [21]. We optimize our guiding function such that the energy is minimal. We found this optimization scheme to be more stable than the usual optimization with respect to the variance. Our results are almost unaffected by small variations in the values of b_{Ne} and b_{ee}, therefore this rather simple procedure is sufficient. For a detailed discussion of more advanced methods for the optimization of Jastrow trial functions see, e.g. [33, 34].

B. Control of the time-step error

The short-time approximation yields an error of order $\mathcal{O}(\delta\tau^2)$, but with a prefactor that strongly depends on the employed guiding function. As we have to consider many different guiding functions for different elements and several magnetic field strengths, it is not a trivial task to find step sizes $\delta\tau$ such that the time-step error is negligible on the one hand, and on the other, that $\delta\tau$ is as large as possible in order to minimize the correlation of our data.

To minimize the time-step error in all cases, we implemented the modifications to the quantum force proposed by Umrigar et al. [35]. In addition to that, we found $\langle|\ln(G_{\mathrm{B}})|\rangle \lesssim 10^{-3}$ per walker and step to be a good criterion for a suitable step size. This means each walker is copied or deleted in each step with a probability of approximately 0.1%. We implemented a routine that performes very small FPDQMC test runs to determine a step size such that this condition is fulfilled. An example of the dependance of the time step error on the value of $\langle|\ln(G_{\mathrm{B}})|\rangle$ is shown in figure 3. Smaller values of $\langle|\ln(G_{\mathrm{B}})|\rangle$ obviously correspond to smaller time steps.

IV. RESULTS AND DISCUSSION

A. Notation

Throughout the rest of this work we will use the high-field notation $(-m,\nu)$ with the magnetic quantum number m and the longitudinal excitation number ν to denote single particle electronic configurations. Corresponding low-field quantum numbers can be found e.g. in [7]. Since FPDQMC works in full configuration space, single particle quantum numbers are replaced by the total wave function's quantum numbers

$$M = \sum_i^N m_i, \quad \Pi_z = \prod_i^N \pi_{z_i}, \quad S_z = \sum_i^N m_{s_i}, \qquad (23)$$

namely the total magnetic quantum number M, the total z-parity Π_z and the total spin-projection S_z. The FPDQMC-method is limited to the computation of the ground state energy of a symmetry subspace $(-M,\Pi_z,-S_z)$ defined by the guiding wave function. Thus, a direct comparison of energies obtained with Hartree-Fock calculations to FPDQMC results is restricted to ground states.

B. Helium

We begin this discussion introducing results for two helium states given in Tables I and II, where we compare our previous results [25] (HFFER) with the ones found by our 2DHFR- and FPDQMC-methods, as well as with 1D Hartree-Fock results from Jones & Ortiz [36], who used an anisotropic basis set, and with those from Thirumalai & Heyl [13], who solved 2D Hartree-Fock equations on a grid.

Compared to our previous HFFER-method, we achieve large improvements for the energy values, especially at small β_Z. Even for very large values of β_Z, there is still a small energy correction to the previous values, since the $(0,0)$ single electron state has a non-vanishing probability density at the nucleus and thus the wave function always retains a small radial symmetric component. For $\beta_Z < 1$, the results from [13] are better than our FPDQMC results. This is due to the phase-error of the 2DHFR guiding function, which cannot be overcome by the FPDQMC-method. For $\beta_Z > 1$ our Hartree-Fock results are in good agreement with both references [13] and [36], and our FPDQMC-results outmatch them both. We note that the 2DHFR program runtime for helium and helium-like ions is about 20 seconds on a single 2.4 GHz AMD Athlon X2 processor.

C. Ground states for $Z = 2$–26

Ground states are of great importance for many applications, e.g. the calculation of ionization energies or ther-

β_Z	HFFER	2DHFR	FPDQMC	Ref.[36]	Ref.[13]
0.1	5.049	5.544	5.6667(3)	5.6602	5.6756
0.2	6.173	6.549	6.6145(2)	6.6032	6.6340
0.5	8.268	8.572	8.6101(1)	8.5960	8.6200
0.7	9.273	9.564	9.5980(1)	9.5822	9.6116
1	10.504	10.784	10.8171(1)	10.800	10.8104
2	13.455	13.722	13.7545(1)	13.733	13.7536
5	18.716	18.969	19.0091(1)	18.976	19.0008
7	21.109	21.357	21.4026(2)	21.3632	21.3896
10	23.956	24.197	24.2494(2)	24.2022	24.2172
20	30.307	30.736	30.8073(2)	30.7380	–
50	41.438	41.777	41.8902(4)	41.7752	–
70	46.310	46.620	46.7514(5)	46.6132	–
100	51.985	52.265	52.4221(6)	52.2528	–

TABLE I. Binding energies of the $(0,0)\,(1,0)$ state of helium – symmetry subspace (1,+,1) – in Rydberg units at different magnetic field strengths calculated with our previous (HFFER) and current (2DHFR, FPDQMC) ansatz, compared to results of other groups.

β_Z	HFFER	2DHFR	FPDQMC	Ref.[36]	Ref.[13]
0.1	4.763	5.245	5.3783(4)	5.3742	5.4040
0.2	5.781	6.140	6.2091(3)	6.2010	6.2392
0.5	7.667	7.953	7.9908(1)	7.9780	8.0036
0.7	8.577	8.849	8.8839(1)	8.8684	8.8984
1	9.696	9.957	9.9910(1)	9.9732	9.9924
2	12.394	12.642	12.6765(1)	12.654	12.6740
5	17.234	17.469	17.5133(1)	17.477	17.4960
7	19.445	19.674	19.7241(2)	19.681	19.7072
10	22.079	22.302	22.3597(2)	22.3080	22.3404
20	27.951	28.406	28.4480(2)	28.3750	–
50	38.330	38.683	38.7795(4)	38.6572	–
70	42.882	43.202	43.3222(5)	43.1908	–
100	48.191	48.478	48.6337(7)	48.4566	–

TABLE II. Binding energies of the $(0,0)\,(2,0)$ state of helium – symmetry subspace (2,+,1) – in Rydberg units at different magnetic field strengths calculated with our previous (HFFER) and current (2DHFR, FPDQMC) ansatz, compared to results of other groups.

mal occupation, and we therefore focus on the computation of their binding energies in this work. We compare our results to the data of heavier atoms in strong magnetic fields obained by Mori and Hailey [12] and Ivanov and Schmelcher [11]. Due to a small error in the code of [22] their results are biased towards lower energies, we therefore exclude them from the comparison.

We list values for the ground states of all atoms from helium to silicon at magnetic field strength 10^7 T (Table IV) and for all atoms from helium to iron at magnetic field strengths $5 \cdot 10^7$ T (Table V), 10^8 T (Table VI) and $5 \cdot 10^8$ T (Table VII), also comparing to our results obtained with the HFFER method. Since those tables display an increasing nuclear charge Z at a fixed magnetic field strength β, β_Z decreases quadratically from top to bottom of the tables, e.g. in Table V β_Z decreases from roughly 27 at $Z = 2$ to about 0.16 at $Z = 26$. In Table IV, we reach the limit of our 2DHFR approach at $Z = 14$ with $\beta_Z \approx 0.11$.

i	configuration
a	(0,1)
$\bar{a}$	(0,0,↑)(0,1)
b	(0,1)(1,1)
$\bar{b}$	(0,0,↑)(0,1)(1,1)
c	(0,1)(1,1)(2,1)
$\bar{c}$	(0,0,↑)(0,1)(1,1)(2,1)
d	(0,1)(1,1)(2,1)(3,1)
D	(0,1)(1,1)(2,1)(0,2)
E	(0,1)(1,1)(2,1)(3,1)(0,2)
F	(0,1)(1,1)(2,1)(3,1)(4,1)(0,2)
$\bar{E}$	(0,0,↑)(0,1)(1,1)(2,1)(3,1)(0,2)
$\bar{F}$	(0,0,↑)(0,1)(1,1)(2,1)(3,1)(4,1)(0,2)

TABLE III. Ground state electronic configuration given in format $(-m, \nu)$ for those electrons that deviate from tightly-bound positions. No index corresponds to the all-tightly-bound high-field ground state.

Table III contains the electronic configurations of all ground states corresponding to the superscripts in Tables IV – VII. The quantum numbers listed only correspond to those electrons with $\nu \neq 0$, while the other electrons occupy tightly-bound orbitals ($\nu = 0$) with falling magnetic quantum numbers m, beginning at $m = 0$. Configurations including only quantum numbers $\nu = 1$ are denoted by lowercase letters, such containing an electron with $\nu = 2$ are denoted by capital letters. All electrons have their spin aligned antiparallel to the magnetic field (↓), except a single electron at (0,0), which may have its spin aligned parallel. If this is the case, it is denoted by (0,0,↑). Configurations including this spin-flipped state electron have overlined letters and were found to form the ground state at $B = 10^7$ T for elements with nuclear charge $Z \geq 11$, and at $B = 5 \cdot 10^7$ T for the heavier elements with nuclear charge $Z = 22$ to 26. Thus, our energy values for these ground states by far excel any result published before.

Throughout all four Tables IV – VII one can notice a significant improvement on the results gained by the 2DHFR method presented in this work compared to the data obtained with the HFFER method. The ground state configuration was found to be the same for both methods. Our results are in goodagreement with those of [11].

It is interesting to note that the relative improvement of the FPDQMC results compared to the 2DHFR-values in the case $B = 5 \cdot 10^8$ T decreases with rising nuclear charge numbers, although the systems grow more complicated due to the larger number of electrons (e.g. for iron FPDQMC only improves the 2DHFR energy by 0.9‰ at this field strength). This effect also occurs at other field strengths but is masked by the growing error of the 2DHFR's Landau expansion that starts to dominate as β_Z falls below 1. However, the FPDQMC results are not affected as severely by this error in the wave function,

Z	HFFER	2DHFR	FPDQMC	Ref.[11]	Ref.[12]
2	19.13	19.38	19.42776(14)	19.39	19.21
3	39.07	39.70	39.7824(3)	39.72	39.23
4	64.80	65.97	66.1171(4)	66.03	65.39
5	95.89	97.81	98.0428(6)	97.92	97.53
6	132.07	134.95	135.3104(8)	135.16	136.27
7	173.10	177.21	177.7634(12)	177.58	–
8	220.01^{a}	225.94^{a}	226.856(2)	226.56^{a}	–
9	272.52^{a}	280.51^{a}	281.796(3)	281.47^{a}	–
10	329.86^{a}	340.38^{a}	342.159(4)	341.83^{a}	–
11	$394.20^{\bar{a}}$	$418.13^{\bar{a}}$	422.164(14)	–	–
12	$477.41^{\bar{b}}$	$508.23^{\bar{b}}$	513.86(2)	–	–
13	$566.55^{\bar{b}}$	$605.37^{\bar{b}}$	612.96(4)	–	–
14	$661.31^{\bar{c}}$	$709.66^{\bar{c}}$	719.94(6)	–	–

TABLE IV. Ground state binding energies in Rydberg units at 10^7 T from helium to silicon calculated with our previous (HFFER) and current (2DHFR, FPDQMC) method, compared to those of other groups. Superscripts denote electronic configuration (see Table III).

and thus the relative energy corrections of FPDQMC to 2DHFR rise again for $\beta_Z \leq 1$, as can be seen in Tables IV – VI.

We performed additional computations at $B = 5{\cdot}10^8$ T to gain a better understanding of this phenomenon. Ee compared the influence of Jastrow factors and the overall correction in FPDQMC of the energy values for all helium-like ions and several iron ions. The results of these computations show a strongly decreasing influence of the electron-electron Jastrow factor with increasing core charge, which can, at least partly, explain this phenomenon.

Compared to the perturbative method of Mori and Hailey [12] we obtain much higher binding energies for small nuclear charges $Z \leq 10$, but for heavier elements and when β_Z falls below 1, their results drop far below even our FPDQMC results, with some ground state configurations differing from the ones found by us. We expect that, in this regime, the method presented in [12] fails to achieve accurate results, as the authors themselves state that its application is limited to $\beta_Z > 2$. We also note that their method is not ab initio and therefore need not neccessarily producee an upper bound on the energy. Our method however, is far from its limit $\beta_Z \geq 0.1$, and our results are to be expected very accurate.

D. Transitions

Transition energies and oscillator strengths are key prerequisites in the analysis of spectra, the only observable quantity of distant stars. The dimensionless oscillator strength f of a transition from an initial state Ψ_i to a final state Ψ_f can be acquired using the well-known relation (see [7])

Z	HFFER	2DHFR	FPDQMC	Ref.[11]	Ref.[12]
2	33.6	33.86	33.9368(3)	33.86	33.6
3	70.1	70.68	70.8405(6)	70.69	70.0
4	117.7	118.77	119.0077(7)	118.79	117.6
5	175.4	177.17	177.4887(8)	177.21	175.7
6	242.6	245.16	245.5660(10)	245.22	243.1
7	318.5	322.17	322.7021(13)	322.28	319.9
8	402.9	407.80	408.4447(13)	407.94	405.5
9	495.4	501.60	502.4218(17)	501.84	500.0
10	595.5	603.30	604.3479(18)	603.69	602.5
11	703.6^{a}	713.46^{a}	714.8493(22)	–	714.3
12	822.0^{a}	$834.03a$	835.682(4)	–	838.6^{a}
13	948.1^{a}	962.61^{a}	964.533(4)	–	973.9^{a}
14	1081.8^{a}	1099.0^{a}	1101.256(5)	–	1120.6^{b}
15	1225.1^{b}	1245.6^{b}	1248.356(6)	–	–
16	1376.2^{b}	1400.1^{b}	1403.384(8)	–	–
17	1534.6^{b}	1562.3^{b}	1566.104(8)	–	–
18	1702.4^{c}	1734.5^{c}	1739.008(1)	–	–
19	1877.5^{c}	1914.2^{c}	1919.484(12)	–	–
20	2060.2^{d}	2102.1^{d}	2108.32(4)	–	–
21	2251.0^{E}	2306.6^{E}	2313.72(6)	–	–
22	$2449.6^{\bar{e}}$	$2549.0\bar{E}$	2563.26(12)	–	–
23	$2660.1^{\bar{e}}$	$2805.6\bar{E}$	2822.02(14)	–	–
24	$2876.2^{\bar{e}}$	$3071.9\bar{E}$	3091.4(16)	–	–
25	$3100.2^{\bar{f}}$	$3348.7\bar{F}$	3370.9(4)	–	–
26	$3331.1^{\bar{f}}$	$3636.6\bar{F}$	3660.4(6)	–	–

TABLE V. Ground state binding energies in Rydberg units at $5{\cdot}10^7$ T from helium to iron calculated with our previous (HFFER) and current (2DHFR, FPDQMC) method, compared to those of other groups. Superscripts denote the electronic configuration (see Table III).

$$f = \Delta E_\mathrm{if} \left| p^q_\mathrm{if} \right|^2 , \tag{24}$$

with the energy difference $\Delta E_\mathrm{if} = E_\mathrm{f} - E_\mathrm{i}$ given in Rydberg units and the total magnetic quantum number difference $q = \Delta M = M_\mathrm{f} - M_\mathrm{i}$ between initial and final state. Since $\Delta M = 0$ transitions are the strongest ones at high magnetic field strengths, we restrict ourselves to the dipole matrix element p^0_if of a photon with linear polarization

$$p^0_\mathrm{if} = \sum_{a,b=1}^{N} \langle \psi^\mathrm{f}_a \left| z \right| \psi^\mathrm{i}_b \rangle C^\mathrm{if}_{ab}. \tag{25}$$

Here C^if_{ab} denotes the cofactor of the single electron wave function overlap matrix S^if_{ab} of initial and final state

$$S^\mathrm{if}_{ab} = \langle \psi^\mathrm{f}_a | \psi^\mathrm{i}_b \rangle. \tag{26}$$

The amount of accurate data for oscillator strengths and transition energies in the literature is small in the literature. In Table VIII. we compare our oscillator strengths with those from Mori and Hailey [12] Since the FPDQMC method is restricted to the calculation of ground states, we can only obtain transitions with the

Z	HFFER	2DHFR	FPDQMC	Ref.[11]	Ref.[12]
2	42.4	42.6	42.7488(6)	42.63	42.4
3	89.5	90.0	90.2140(10)	89.99	89.2
4	151.3	152.4	152.6872(12)	152.37	151.1
5	226.8	228.5	228.9330(12)	228.53	226.7
6	315.0	317.5	318.020(2)	317.51	315.2
7	415.0	418.5	419.147(2)	418.55	415.8
8	526.3	531.0	531.721(3)	531.02	527.4
9	648.3	654.3	655.200(4)	654.40	650.1
10	780.5	788.1	789.160(2)	788.24	783.8
11	922.7	931.9	933.204(3)	–	927.9
12	1074.4	1085.5	1086.978(4)	–	1083.7
13	1235.3	1248.5	1250.216(4)	–	1247.5^a
14	1409.6^a	1425.6^a	1427.764(6)	–	1426.5^a
15	1593.5^a	1612.2^a	1614.580(6)	–	1616.0^a
16	1786.8^a	1808.3^a	1811.032(6)	–	1816.7^b
17	1990.9^b	2015.9^b	2019.118(8)	–	2029.9^b
18	2205.8^b	2234.3^b	2237.902(8)	–	2261.3^b
19	2429.9^b	2462.1^b	2466.186(10)	–	2501.6^b
20	2664.1^c	2700.7^c	2705.37(3)	–	2756.2^c
21	2909.0^c	2950.0^c	2955.248(3)	–	–
22	3162.7^c	3208.5^c	3214.16(4)	–	–
23	3426.7^d	3477.8^d	3484.24(4)	–	–
24	3700.4^d	3757.1^d	3764.24(6)	–	–
25	3983.3^E	4054.4^E	4062.54(8)	–	–
26	4277.7^E	4357.2^E	4366.14(10)	–	–

TABLE VI. Ground state binding energies in Rydberg units at 10^8 T from helium to iron calculated with our previous (HFFER) and current (2DHFR, FPDQMC) method, compared to those of other groups. Superscripts denote the electronic configuration (see Table III).

Z	HFFER	2DHFR	FPDQMC	Ref.[11]	Ref.[12]
2	70.6	70.7	70.9782(16)	70.70	70.37
3	153.2	153.6	154.108(4)	153.56	152.73
4	264.6	265.5	266.134(4)	265.35	263.57
5	402.9	404.4	405.210(6)	404.21	402.48
6	566.5	568.7	569.748(6)	568.53	565.57
7	754.0	757.2	758.368(8)	756.98	751.96
8	964.4	968.6	969.962(10)	968.38	962.76
9	1196.4	1202.0	1203.510(8)	1201.70	1195.38
10	1449.4	1456.3	1458.144(8)	1456.06	1448.07
11	1722.3	1730.9	1732.922(10)	–	1720.31
12	2014.7	2025.1	2027.306(8)	–	2016.51
13	2325.8	2338.1	2340.490(8)	–	2328.07
14	2655.0	2669.4	2672.072(8)	–	2657.27
15	3001.8	3018.4	3021.418(10)	–	3007.2
16	3365.7	3384.8	3388.112(10)	–	3372.19
17	3746.3	3768.0	3771.580(14)	–	3753.36
18	4143.2	4167.7	4171.518(10)	–	4154.88
19	4555.9	4583.4	4587.51(3)	–	4570.22
20	4984.3	5014.9	5019.49(2)	–	5000.19
21	5434.2^a	5468.7^a	5473.92(4)	–	5452.42^a
22	5901.4^a	5939.6^a	5945.02(4)	–	5924.14^a
23	6384.3^a	6426.3^a	6432.08(6)	–	6413.71^a
24	6882.6^a	6928.6^a	6934.72(6)	–	6927.91^a
25	7401.0^b	7451.8^b	7458.64(4)	–	7441.74^a
26	7936.3^b	7991.7^b	7998.84(6)	–	7984.89^b

TABLE VII. Ground state binding energies in Rydberg units at $5 \cdot 10^8$ T from helium to iron calculated with our previous (HFFER) and current (2DHFR, FPDQMC) method, compared to those of other groups. Superscripts denote the electronic configuration (see Table III).

2DHFR method, but the small corrections of FPDQMC compared to the 2DHFR results for the energy values make us to expect that the results for oscillator strengths are very accurate as well.

The new results are in good agreement with those obtained with our previous version of the Hartree-Fock-Roothaan method (HFFER): the largest differences in oscillator strength and energy (about 7% and 2.6%, respectively) can be found at the transition of the innermost electron $m = 0$ at the lowest magnetic field strength $\beta = 200$. Here, the inital single particle (0,0)-state is signficantly improved by our new 2D expansion, while the final (0,1)-state has a node at $z = 0$ and thus can be described adequately well by both expansions (2) and (3). When the error of both the inital and final single electron state is of the same order even expansion (2) proves to be useful and predicts transition energies and oscillator strengths properly, as can be seen looking at the transitions of $m = 5$.

Comparing our oscillator strengths to the results of [12], one can see quite big differences for all transitions, with a maximum difference of 27%. The authors of [12] mention lacking orthogonality of inital and final state and only calculate the dipole matrix element for the electron that undergoes a transition. This may explain the large discrepancies. Since we evaluate formula (25) exactly and work with perfectly orthogonal states, our results should be the more accurate ones..

V. SUMMARY AND OUTLOOK

In this work we have presented an approach for the very accurate calculation of ground state energy levels of atoms in strong and intermediate magnetic fields of $\beta_Z \geq 0.1$, combining 2D-Hartree-Fock-Roothaan and fixed-fhase diffusion Monte Carlo methods. The results shown for helium states at different magnetic field strengths and all element ground states from helium up to iron show the efficiency and accuracy of our approach. Including the spin-flipped (0,0,↑) single electron state into possible ground state configurations we found new ground states for sodium to silicon at $B = 10^7$ T and titanium to iron at $B = 5 \cdot 10^7$ T.

The applied 2DHFR method was optimized to reduce the calculation effort originating from electron-electron interaction intergrals, while at the same time the single particle Landau expansion was boosted, thus increasing the overall precision. We demonstrated that the induced additional errors stay very small, resulting in good convergence behaviour of this method. In addition it also allows for the calculation of excited states and electronic

	$\beta = 200$			$\beta = 500$			$\beta = 1000$		
m	HFFER	2DHFR	Ref.[12]	HFFER	2DHFR	Ref.[12]	HFFER	2DHFR	Ref.[12]
0	1024	1051	–	1370	1394	–	1696	1718	–
	(42.0)	(45.4)	(41.0)	(12.0)	(12.5)	(13.0)	(6.2)	(6.3)	(5.81)
1	481	485	–	671	675	–	854	858	–
	(68.4)	(70.4)	(59.8)	(27.1)	(27.4)	(22.5)	(15.5)	(15.7)	(12.8)
2	314	315	–	447	448	–	576	577	–
	(99.9)	(101.2)	(79.7)	(45.7)	(46.0)	(39.2)	(27.7)	(27.8)	(24.7)
3	233	233	–	335	335	–	435	436	–
	(135.8)	(136.6)	(114.)	(67.9)	(68.1)	(61.1)	(42.4)	(42.5)	(37.7)
4	180	180	–	262	262	–	343	344	–
	(173.2)	(173.7)	(156.)	(93.0)	(93.1)	(86.3)	(59.9)	(59.9)	(57.2)
5	132	132	–	195	196	–	259	259	–
	(205.5)	(205.8)	(197.)	(119.9)	(120.0)	(116.)	(80.5)	(80.5)	(78.3)

TABLE VIII. Transition energies in eV and oscillator strengths $\cdot 10^{-3}$ (in brackets) of $\Delta M = 0$ bound-bound transitions from electrons $(-m, \nu = 0)$ of the ground state of neutral carbon to $(-m, \nu = 1)$, at three different magnetic field strengths β compared to results from Mori et al. [12].

wave functions which were directly applied to obtain oscillator strengths for atomic bound-bound transitions and were used as guiding wave functions for even more precise FPDQMC calculations.

The comparison with results in the literature for elements $Z \leq 10$ shows that the accuracy of our Monte Carlo approach can very well compete with other precise methods, while also allowing for the treatment of elements with $Z = 10 - 26$. This makes FPDQMC, especially in the combination with our 2DHFR approach, a tool well suited for the study of the on symmetry subspace ground states of mid-Z elements in strong magnetic fields.

We note that the self-healing diffusion quantum Monte Carlo algorithms proposed recently by Reboredo et al. [31, 32] and a method for the calculation of excited states from full configuration interaction Monte Carlo presented by Booth and Chan [37] may be worthwhile avenues to pursue in future work on atoms in strong magnetic fields.

ACKNOWLEDGMENTS

This work was supported by Deutsche Forschungsgemeinschaft. We gratefully thank the bwGRiD project [38] for the computational resources.

[1] F. Haberl, A. D. Schwope, V. Hambaryan, G. Hasinger, and C. Motch, A&A **403**, L19 (2003).
[2] V. Hambaryan, R. Neuhäuser, F. Haberl, M. M. Hohle, and A. D. Schwope, A&A **497**, L9 (2009).
[3] V. Hambaryan, V. Suleimanov, A. D. Schwope, R. Neuhäuser, K. Werner, and A. Y. Potekhin, A&A **534**, A74 (2011).
[4] *Neutron stars and pulsars*, edited by W. Becker, Astrophysics and Space Science Library, Vol. 357 (Springer-Verlag, 2009) ISBN 978-3-540-76965-1.
[5] B. Külebi, S. Jordan, F. Euchner, B. T. Gänsicke, and H. Hirsch, A&A **506**, 1341 (2009).
[6] S. O. Kepler, I. Pelisoli, S. Jordan, S. J. Kleinman, D. Koester, B. Külebi, V. Peçanha, B. G. Castanheira, A. Nitta, J. E. S. Costa, D. E. Winget, A. Kanaan, and L. Fraga, Mon. Not. R. Astron. Soc. **429**, 2934 (March 11, 2013).
[7] H. Ruder, G. Wunner, H. Herold, and F. Geyer, *Atoms in Strong Magnetic Fields*, A&A Library (Springer-Verlag, 1994) ISBN 3-540-57699-1.
[8] L. B. Zhao and P. C. Stancil, J. Phys. B **40**, 4347 (2007).
[9] Y. P. Kravchenko, M. A. Liberman, and B. Johansson, Phys. Rev. A **54**, 287 (Jul 1996).
[10] Y. P. Kravchenko, M. A. Liberman, and B. Johansson, Phys. Rev. Lett. **77**, 619 (Jul 1996).
[11] M. V. Ivanov and P. Schmelcher, Phys. Rev. A **61**, 022505 (Jan. 2000).
[12] K. Mori and C. J. Hailey, ApJ **564**, 914 (2002).
[13] A. Thirumalai and J. S. Heyl, Phys. Rev. A **79**, 012514 (2009).
[14] X. Guan and B. Li, Phys. Rev. A **63**, 043413 (2001).
[15] X. Guan, B. Li, and K. T. Taylor, J. Phys. B **36**, 2465 (2003).
[16] O. A. Al-Hujaj and P. Schmelcher, Phys. Rev. A **70**, 033411 (Sep. 2004).
[17] O. A. Al-Hujaj and P. Schmelcher, Phys. Rev. A **70**, 023411 (Aug. 2004).
[18] X. Wang and H. Qiao, Phys. Rev. A **75**, 033421 (2007).
[19] X. Wang and H. Qiao, Phys. Rev. A **80**, 053425 (2009).
[20] X. Wang and H. Qiao, Few-Body Syst. **53**, 453 (2009).
[21] B. L. Hammond, W. A. Lester, jr., and P. J. Reynolds, *Monte Carlo Methods in ab initio quantum chemistry*, World Scientific Lecture and Course Notes in Chemistry (World Scientific Publishing Co. Pte. Ltd., Singa-

pur, 1994).
[22] S. Bücheler, D. Engel, J. Main, and G. Wunner, Phys. Rev. A **76**, 032501 (2007).
[23] M. D. Jones, G. Ortiz, and D. M. Ceperley, Phys. Rev. E **55**, 6202 (May 1997).
[24] D. Meyer, S. Boblest, and G. Wunner, Phys. Rev. A **87**, 032515 (Mar 2013).
[25] D. Engel and G. Wunner, Phys. Rev. A **78**, 032515 (2008).
[26] C. Schimeczek, D. Engel, and G. Wunner, Comp. Phys. Comm. **183**, 1502 (Jul. 2012).
[27] C. de Boor, J. Approx. Theory **6**, 50 (1972).
[28] W. M. C. Foulkes, L. Mitas, R. J. Needs, and G. Rajagopal, Rev. Mod. Phys. **73**, 33 (Jan 2001).
[29] A. Lüchow, Comput. Mol. Sci. **1**, 388 (2011).
[30] G. Ortiz, D. M. Ceperley, and R. M. Martin, Phys. Rev. Lett. **71**, 2777 (Oct. 1993).
[31] F. A. Reboredo, R. Q. Hood, and P. R. C. Kent, Phys. Rev. B **79**, 195117 (2009).
[32] F. A. Reboredo, J. Chem. Phys. **136**, 204101 (2012).
[33] J. Toulouse and C. J. Umrigar, J. Chem. Phys. **128**, 174101 (2008).
[34] H. Luo, J. Chem. Phys. **135**, 024109 (2011).
[35] C. J. Umrigar, M. P. Nightingale, and K. J. Runge, J. Chem. Phys. **99**, 2865 (1993).
[36] M. D. Jones, G. Ortiz, and D. M. Ceperley, Phys. Rev. A **59**, 2875 (Apr. 1999).
[37] G. H. Booth and G. K. Chan, J. Chem. Phys. **137**, 191102 (2012).
[38] bwGRiD (http://www.bw-grid.de/), *Member of the German D-Grid initiative, funded by the Ministry of Education and Research (Bundesministerium für Bildung und Forschung) and the Ministry for Science, Research and Arts Baden-Wuerttemberg (Ministerium für Wissenschaft, Forschung und Kunst Baden-Württemberg)*, Tech. Rep. (Universities of Baden-Württemberg, 2007-2013).